Research on
Engineering
Structures & Materials
journal homepage: http://jresm.org

RESEARCH
GROUP

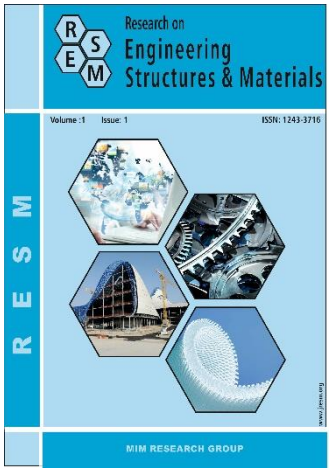

Mass effect on magnetic flux behavior

Deniz Perin, Aykut Ilgaz, Mustafa Göktepe

Online Publication Date: 25 Mar 2016
URL: ttp://dx.doi.org/10.17515/resm2015.31ma1230.html
DOI: ttp://dx.doi.org/10.17515/resm2015.31ma1230

Journal Abbreviation: *Res. Eng. Struct. Mat.*

To cite this article
Perin D, Ilgaz A, Göktepe M. Mass effect on magnetic flux behavior. *Res. Eng. Struct. Mat.*, 2017; 3(2): 147-153

Research on
Engineering
Structures & Materials
journal homepage: http://jresm.org

RESEARCH GROUP

Research Article

Mass effect on magnetic flux behavior

Deniz Perin, Aykut Ilgaz*,1, Mustafa Göktepe[1]

[1]*Department of Physics, Balikesir University, Balikesir, Turkey*

Article Info

Article history:
Received 30 Dec 2015
Revised 24 Mar 2016
Accepted 25 Mar 2016
Keywords:
Magnetic flux
Magnetic induction
Mass effect

Abstract

The behavior of the magnetic flux on ferromagnetic samples has been investigated using Magnetic Flux Leakage (MFL) technique in this paper. The magnetic flux distribution was revealed by analysis of the MFL signals. Also, magnetic flux lines detected by sensor have been exhibited visually with simulation illustrations. This work introduces how variation in the mass and length of the magnetic sample effects magnetic flux distribution both experimentally and theoretically.

1. Introduction

Magnetic Flux Leakage (MFL) testing is one of the most widely used Non-Destructive Technique (NDT) which is commonly applied for various industrial sectors such as pipelines, tubes, railways, automotive, steel industry [1-4]. Due to this, physics of magnetic flux phenomena observed on ferromagnetic materials is well known and still continues to be described in number of studies [5-11]. The raw data needs to process in MFL technique. Therefore, with the development of the MFL signal processing technology, the inspection efficiency has been increased in recent years [12]. Another factor that increases the quality of the inspection is sensor system. The new several sensors such as superconducting quantum interference device (SQUID) [13], giant magneto resistance (GMR) [14] have been introduced to increase sensitivity and resolution of testing. MFL still continues to attract attention with these developments although there are many inspection methods.

In this work, the behavior of magnetic flux on SiFe laminated specimen is discussed using MFL technique. Firstly, response of magnetic flux to the increase in sample mass is investigated experimentally. Similarly, the variation of magnetic induction depending on the length of the sample is examined in the second section. These experimental results are confirmed with theoretical fits.

2. Theoretical Background

MFL is a well-known research area. MFL is not only a research area but also used in commercial industrial applications. This makes it an attractive point of MFL. The results are easy to understand but background of MFL is a bit complicated. So many approximations have been done to make it clear. The most known of these studies was done by Lord *et al* [15]. Shcherbinin and Pashagin extended low dimensional defects model to three dimensional models [16]. Edwards and Palmer proposed dipole strength with the magnetizing conditions of the sample [17]. They introduced an analytical solution for the magnetic flux behavior as a function of the applied magnetic field via

*Corresponding author: aykut17ilgaz@gmail.com
DOI: http://dx.doi.org/10.17515/resm2015.31ma1230

$$H_x = \int_{-b}^{0}\int_{-c}^{+c} \frac{\sigma_s x\,\partial z'\,\partial y'}{4\pi[x^2+(z-z')^2+(y-y')^2]^{3/2}} \quad (1)$$

$$H_y = \int_{-c}^{+c}\int_{-b}^{0} \frac{\sigma_s y\,\partial y'\,\partial z'}{4\pi[x^2+(y-y')^2+(z-z')^2]^{3/2}} \quad (2)$$

$$H_z = \int_{-b}^{0}\int_{-c}^{+c} \frac{\sigma_s (z-z')\,\partial z'\,\partial y'}{4\pi[x^2+(y-y')^2+(z-z')^2]^{3/2}} \quad (3)$$

The characteristic MFL crack signal can be figured out with these equations where x, y, z are related with the sample, and a, b, c are related with the crack dimension.

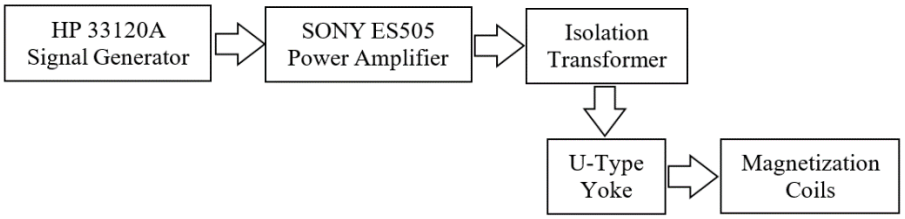

Fig. 1 Magnetizing system schematic diagram

Experimental setup consists of magnetizing system and sensor system in order to capture MFL signals. The magnetizing system has HP 33120A signal generator, SONY ES505 power amplifier, isolation transformer, U-type yoke, two magnetization coils as shown in Fig. 1. The signal generator produces the sinusoidal signal which was increased to 2 Ampere by power amplifier. The amplified signal was magnetized the laminated sheet and the sensor captured magnetic flux on the sheet which converse the flux to analog signal.

The signal from data logger was gathered by interface board and recorded in computer. The sensor was also placed on moving shaft that was controlled by a driven step motor as shown in Fig. 2. The flux lines were detected by this sensor system traveling throughout on the sample. The graphics are obtained by the sensor voltage versus sample length with the recorded data.

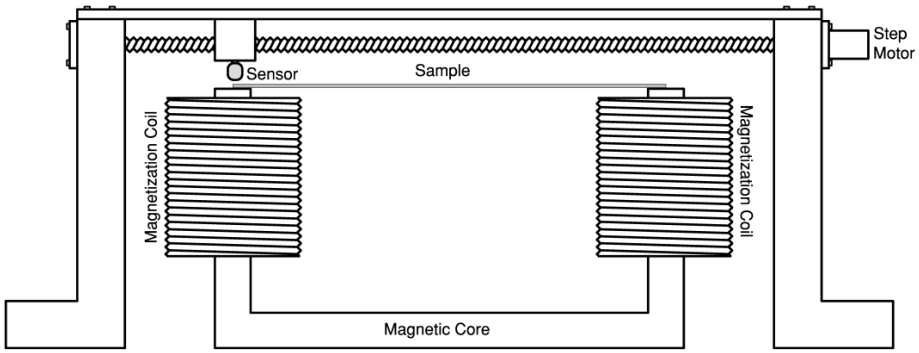

Fig. 2 MFL measurement setup

A crack on laminated sheet was measured with the constructed experimental setup. Data agree well with the equations that given above. Instead of crack signal, the variation of magnetic induction with respect to mass of magnetic material was studied in this paper.

3. Experimental Results

The magnetic flux which captured by the sensor, can be changed by discontinuities, impurities and mass of magnetic material. The mass of magnetic material is an important factor for the density of magnetic flux. Numbers of experiments were done between the poles of yoke with different mass of magnetic material to determine the variations of magnetic flux under a constant magnetic field.

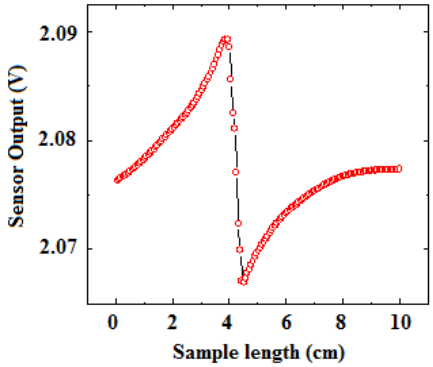

Fig. 3 The rectangular crack signal from Si-Fe laminated sheet.

Sensor captured the highest value on the pole of yoke with no sheet but it dramatically decreases to a minimum value after the pole as shown in Fig. 3. This means measurable magnetic flux density is higher on the poles. When a laminated sheet placed on the poles of yoke, the magnetic flux prefers to travel within the sheet. The magnetic flux which goes through the laminated sheet cause a decline on the sensor value but after the pole, sensor value increases because of the sheet which concentrates magnetic flux around the sheet. The considerable gap occurs between the signals of no sheet and one sheet on the pole and after the pole as shown in Fig. 4. There is no important variation with two sheets so three sheets were placed on the poles of the yoke. The magnetic flux gives the same value on the pole and after the pole with three sheets. Laminated sheet acts like a core of the yoke which concentrates magnetic flux between the poles of the yoke.

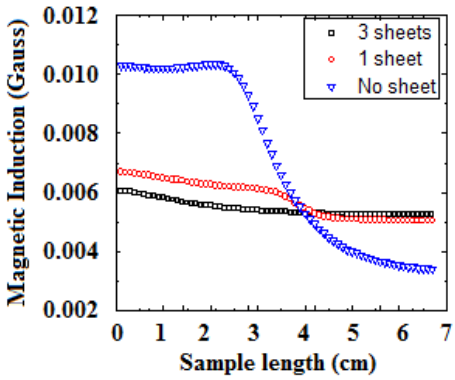

Fig. 4 Experimental results at the pole of yoke with no sheet, 1 sheet and 3 sheets.

The variation of magnetic field lines at pole of yoke is shown as graphics of experimental results and simulation illustrations in Fig. 5. The magnetic flux lines which cause the sensor

output can be seen in illustrations. The only changing quantity is magnetic material mass in three experiments and simulations.

Magnetic flux lines are denser at the corners of the pole. These lines create maximum sensor output in the experiment. The maximum values recorded at the corners of the pole after the corners the sensor output decreases with exponential function as

$$y = y_0 + \left(\frac{A}{B\sqrt{\pi/4\ln 2}}\right) \exp\left(-4\left(\frac{x-C}{B}\right)^2\right) \quad (4)$$

When a laminated sheet placed on the inner corner of the yoke magnetic flux lines penetrate into the sheet and magnetize it. Sensor output is lower than outside corner of the pole because of the flux penetration. The graphic changes by a new exponential function expressed as follows:

$$y = y_0 + A.\exp\left(-0.5\left(\frac{x-C}{B}\right)^2\right) \quad (5)$$

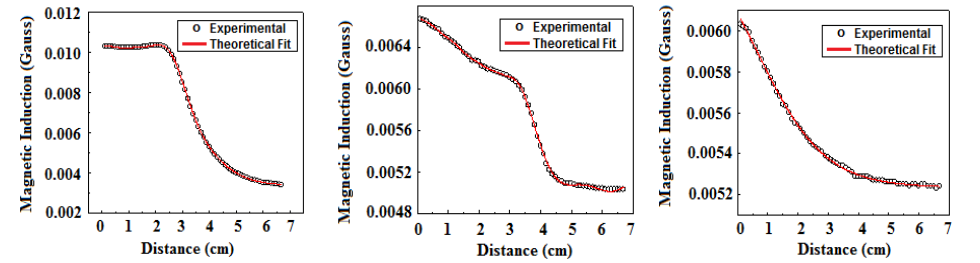

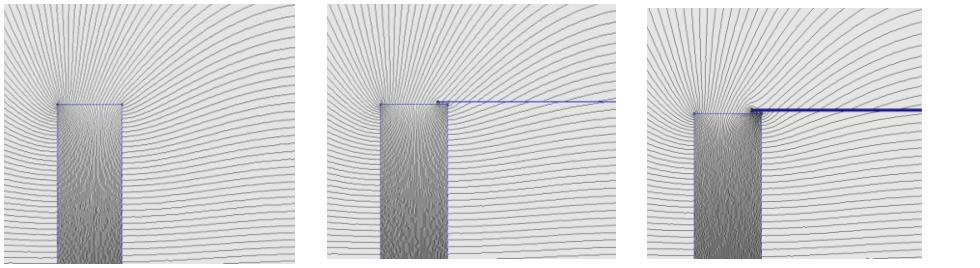

(a) no sheet on the pole **(b)** one sheet on the pole **(c)** three sheets on the pole

Fig. 5. The variation of magnetic field lines at pole of yoke as graphics of experimental results and simulation

The magnetic flux lines, which penetrate into the three laminated sheets, lose their effects on the sensor output at the corner of the yoke. In another words all flux lines leak in the sheet so sensor output decreases dramatically and can be given with the function

$$y = y_0 + \left(\frac{A\text{-}y_0}{1+\exp\left(\frac{x-B}{C}\right)}\right) \quad (6)$$

where y_0, A, B, C are the computed coefficients for the estimated fit. The estimated coefficients for the three cases are listed in Table 1.

The behavior of magnetic induction related with mass of magnetic material was examined with number of laminated sheets. When the number of sheets increase on the pole, the flux which increased sensor output prefers to travel within the laminated sheet, sensor voltage decreases on the pole as shown in Fig. 5. After exposed this change, the effect of sample

length variation on sensor output was examined. In order to analyze for the variation of magnetic induction with respect to sample length, different length samples placed between legs of the yoke are 65 mm, 125 mm and 220 mm as shown in Fig. 6.

Table 1 The coefficients in the theoretical fits for the different sheet number.

Fitting Coefficients	No sheet	1 sheet	3 sheet
y_0	34.10^{-4}	66.10^{-4}	52.10^{-4}
A	3.10^{-2}	11.10^{-5}	65.10^{-3}
B	14.20	8.18	6.66
C	3.40	0.24	11.08

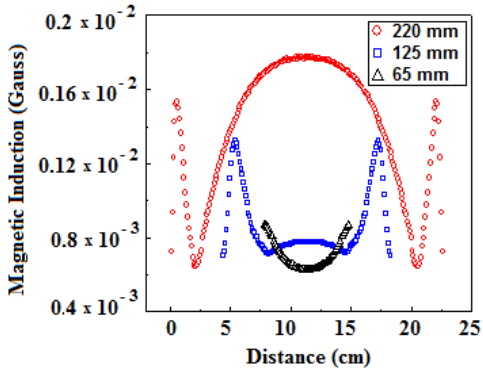

Fig. 6. Comparison of the measured magnetic induction versus distance for different sample length.

It can be seen from the graphic that while the magnetic induction exhibits similar acts at corners of the samples, acts differ towards the centers of the samples. The longest sample makes a major contribution to total magnetization at the middle of the sample exceeding the peak values in the corners. However, when length of the sample is shortened, contribution to total magnetization is reduced dramatically like in 125 mm sample. The sensor outputs in 65 mm sample take minimum at the middle of the sample because magnetic flux lines are not sufficient to magnetize the sample due to its high magnetic susceptibility.

The contribution to the sensor voltage comes from magnetization of the sample as shown in Fig. 7. The sensor captures magnetic induction which changes from B=μH to B=μ(H+M). The flux lines which penetrating into sample at the corners start to magnetize and the magnetized sample increases sensor voltage. Totally, it gives a parabola with a function given as

$$y = y_0 + A \exp\left(-0.5\left(\frac{x-C}{B}\right)^2\right) \quad (7)$$

The fitting constants are y_0 = -15.3, A = 15.3, B = 7701, C = 113.4 for the 220 mm sample.

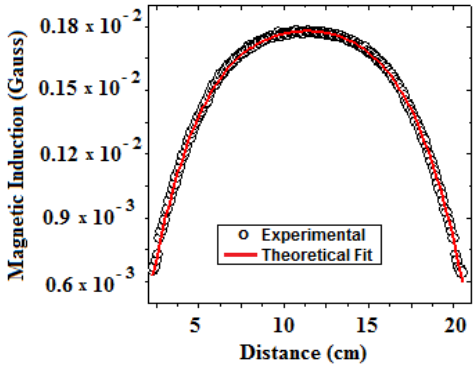

Fig. 7. The sensing experimental magnetic induction and theoretical fit for middle of the 220 mm sample.

The magnetic flux which wants to penetrate into the short magnetic material, are much than the penetrated flux. Therefore the sensor output at the corner is higher than value at the middle of the sample. So the graphic changes to Gaussian in Fig. 8 and given with

$$y = y_0 + \left(\frac{A}{B\sqrt{\pi/2}}\right) \exp\left(-2\left(\frac{x-C}{B}\right)^2\right) \quad (8)$$

where $y_0 = 6.37.10^{-3}$, A = -1.68, B = 237, C = 36.46 are fitting constants.

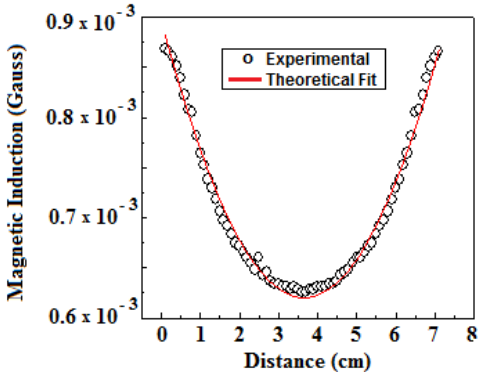

Fig. 8 The sensing experimental magnetic induction and theoretical fit for 65 mm sample.

It is easy to understand, magnetic flux wants to penetrate to magnetic material. Due to its length, the contribution to sensor output changes. The contribution changes from a parabola to Gaussian function which is given above with graphics.

4. Conclusions

In this study, the effects of sample's mass and length on magnetic induction were analyzed. Sensing and processing signal data was supported by the theoretical calculations. It was found that mass and length of the sample were critical parameters affecting the magnetic flux behavior. This paper has been a pioneer work to measure the response of the magnetic induction to length and mass variation of the sample.

Acknowledgments

The research described in this paper was financially supported by the Scientific Research Projects Unit of Balikesir University (1.2015.0054).

References

[1] Crouch AE. In-line inspection of natural gas pipelines. Gas Research Inst. Topical Rep., 1993:12–16.
[2] Tandon KK. MFL tool hardware for pipeline inspection. Materials Selec. Design, 1997:75–79.
[3] Kikuchi H, Kurisawa Y, Ara K, Kamada Y, Kobayashi S. Feasibility study of magnetic flux leakage method for condition monitoring of wall thinning on tube.Int. J. Appl. Elec. and Mech., 2010; 33: 3-4.
[4] Kim JH, Kim MH and Choi DH. Analysis and Depth Estimation of Complex Defects on the Underground Gas Pipelines. Journal of Magnetics, 2013; 18(2):202-206. http://dx.doi.org/10.4283/JMAG.2013.18.2.202
[5] Forster F. Nondestructive inspection by the method of magnetic leakage fields. Defektoskopia, 1982; 11: 3-25.
[6] Edwards C, Palmer SB. The magnetic leakage field of surface breaking cracks. J. Phys. D,1986; 19: 657-73. http://dx.doi.org/10.1088/0022-3727/19/4/018
[7] Cho SH, Yoo HR, Kim DK, Park DJ, Rho YW, Seo K, Park GS, Choi DH and Song SJ. Implementation of High Magnetization System for Performance Enhancement of Magnetic Flux Leakage Tool. Journal of Magnetics, 2010;15(4):199-203. http://dx.doi.org/10.4283/JMAG.2010.15.4.199
[8] Perin D, Göktepe M. Inspection of rebars in concrete blocks. Int. J. Appl. Elec. and Mech., 2012; 38: 2-3.
[9] Zatsepin NN, Shcherbinin VE. Calculation of the magneto static field of surface defects. Defecktoskopiya, 1966; 5: 50-59.
[10] Mandache C, Clapham L. A model for a magnetic flux leakage signal predictions. J. Phys. D, 2003; 36: 2427–2431. http://dx.doi.org/10.1088/0022-3727/36/20/001
[11] Sun Y, Kang Y. A new MFL principle and method based on near-zero background magnetic fields. NDT&E International, 2010; 43: 348–353. http://dx.doi.org/10.1016/j.ndteint.2010.01.005
[12] Mao B, Lu Y, Wu P, Mao B and Li P.Signal processing and defect analysis of pipeline inspection applying magnetic flux leakage methods. Intel Serv Robotics, 2014; 7: 203–209. http://dx.doi.org/10.1007/s11370-014-0158-6
[13] Krause HJ, Kreutzbruck MV. Recent development in SQUID NDE. Physica C, 2002; 368: 70–9. http://dx.doi.org/10.1016/S0921-4534(01)01142-X
[14] Tsukada K, Yoshioka M, Kiwa T, Hirano Y. A magnetic flux leakage method using a magnetoresistive sensor for nondestructive evaluation of spot welds. NDT and E International, 2011; 44: 101–5. http://dx.doi.org/10.1016/j.ndteint.2010.09.012
[15] Lord W and Hwang JH. Br. J. Non-dest. Testing, 1977; 19:14–18.
[16] Shcherbinin VE and Pashagin AI. Defektoskopyia, 1972; 8: 74–82.
[17] Edwards C and Palmer SB. J. Phys. D: Appl. Phys, 1986; 19: 657–73. http://dx.doi.org/10.1088/0022-3727/19/4/018